Efficient Computation of Thin-layer Structures with the Unconditionally Stable ADI-FDTD Method

Chenghao Yuan, *Student Member, IEEE* and Zhizhang Chen, *Senior Member, IEEE*

Microwave Wireless Research Laboratory,
Department of Electrical and Computer Engineering, Dalhousie University,
Halifax, Nova Scotia, Canada B3J 2X4
Email: cyuan@dal.ca and z.chen@dal.ca

Abstract— **Efficient computation is one of the key considerations in computational electromagnetics, especially for complex VLSI structures that contain thin dielectric layers or electrically small objects. Due to the CFL stability condition, it is very inefficient to apply the conventional FDTD method to thin-layer structures because fine mesh (and therefore small time step) is required. In this paper, the unconditionally stable ADI-FDTD method is employed to circumvent the difficulty. With the exemplary applications in computing effective dielectric constant(ε_{eff}) and characteristic impedance (Zo) of cylindrical microstrip lines, it is shown that the computation time with ADI-FDTD method is much shorter than that of conventional FDTD method without scarifying modeling accuracy.**

I. INTRODUCTION

The FDTD method has been proved to be a well-suited tool for solving a variety of electromagnetic problems [1]. In theory, it can be applied to compute the structures with arbitrary medium parameters and shapes. In practice, however, due to the CFL stability condition and numerical dispersion, the FDTD can only be applied to structures that do not require very fine mesh for good accuracy. For a structure with fine mesh, the time step can be so small the total number of iterations and the total simulation time become prohibitively large. As well, a large number of iterations will result in worse or even unacceptable modeling inaccuracy due to the computer-generated errors [2].

On the other hand, with the advancement in MIC/MMIC design and technology, thin film and multilayer structures appear more and more in place of conventional RF and microwave structures. However, modeling of these structures remains difficult with the conventional FDTD method, in particular when a thin film layer or a small object is located in a relatively large structure. Therefore, development of an efficient FDTD simulation scheme without losing modeling accuracy becomes a great challenge in computational electromagnetics.

The recently developed 3-D ADI-FDTD method [3][4] presents a potential candidate for simulating the thin-layer structures where fine mesh has to be applied to parts of the structures. The ADI-FDTD method is unconditionally stable. Therefore, time step can be selected independently from space step [5]. A few ADI-FDTD applications utilizing this property were reported in [6][7][8]. In this paper, the ADI-FDTD is further extended and applied to thin layer structures. Because of our on-going proprietary research projects, cylindrical microstrip structures are chosen as the case of our studies. By demonstrating the effectiveness and efficiency in computing ε_{eff} and Zo of the cylindrical microstrip lines that have large width to thickness ratios, the ADI-FDTD is validated in solving thin-layer structures. With it, a general cylindrical ADI-FDTD formulation for simulating cylindrical open structures is also presented.

This paper is organized in the following manner: Section II gives the newly developed formulation of the cylindrical ADI-FDTD capable of modeling general *open* cylindrical structures with materials of arbitrary conductivity and permittivity. Section III presents the numerical results and analysis. Section IV is the summary and conclusions.

II. NEWLY DEVELOPED FORMULATION OF ADI-FDTD FOR MODELING GENERAL CYLINDRICAL OPEN STRUCTURES

In [9], the authors have presented the formulation of cylindrical ADI-FDTD for solving closed structures. For open structures and scattering problems, a suitable absorbing boundary condition (ABC) has to be incorporated to truncate an open solution domain. Here, the nonsplit uniaxial perfectly matched layers absorbing boundary condition (UPML-ABC) [10] is adapted. Based on [10], Maxwell's equations in UPML medium in the cylindrical coordinates can be found as:

0-7803-7695-1/03/$17.00 © 2003 IEEE

$$\varepsilon\frac{\partial P_r'}{\partial t}+\sigma P_r'=\frac{\partial H_z}{r\partial\phi}-\frac{\partial H_\phi}{\partial z}$$
$$\frac{\partial P_r'}{\partial t}=k_r\frac{\partial P_r}{\partial t}+\frac{\int_0^r\sigma(r)dr}{\varepsilon_0 r}P_r \quad (1)$$
$$k_r\frac{\partial P_r}{\partial t}+\frac{\sigma_r}{\varepsilon_0}P_r=k_z\frac{\partial E_r}{\partial t}+\frac{\sigma_z}{\varepsilon_0}E_r$$

where σ is the background electric conductivities of medium, σ_d (d=r,z) is the directional conductivity in the radial or axial direction in which the cylindrical waves are to be absorbed. P_r and P_r' are the auxiliary field components. $\kappa_d\,(d=r,z)$ can be considered as equivalent to the complex frequency shift of the Complex Frequency Shift constitutive PML (CFS-PML) [11].

By applying the ADI-FDTD principle to the above equations as described in [9], 30 equations can be obtained in two sub iterations for a general 3D case. For instance, equation (1) can be broken into two sub-step computation as in the following:

For the first sub time step:

$$E_r^{n+\frac12}(i+\tfrac12,j,k)=\frac{cz1(i+\frac12,j,k)E_r^n(i+\frac12,j,k)-cr1(i+\frac12,j,k)P_r^n(i+\frac12,j,k)}{cz2(i+\frac12,j,k)}+\frac{cr2(i+\frac12,j,k)\left[crI1(i+\frac12,j,k)P_r^n(i+\frac12,j,k)-P_r'^n(i+\frac12,j,k)\right]}{cz2(i+\frac12,j,k)crI2(i+\frac12,j,k)}+\frac{cr2(i+\frac12,j,k)P_r'^n(i+\frac12,j,k)}{cz2(i+\frac12,j,k)crI2(i+\frac12,j,k)cm(i+\frac12,j,k)}+\frac{\Delta t\cdot cr2(i+\frac12,j,k)}{2\varepsilon\left(i+\frac12,j,k\right)\cdot cz2(i+\frac12,j,k)crI2(i+\frac12,j,k)cm(i+\frac12,j,k)}\left[\frac{H_z^{n+\frac12}(i+\frac12,j+\frac12,k)-H_z^{n+\frac12}(i+\frac12,j-\frac12,k)}{\phi(i+\frac12)\cdot(i+\frac12)\cdot r(i+\frac12)}-\frac{H_\phi^n(i+\frac12,j,k+\frac12)-H_\phi^n(i+\frac12,j,k-\frac12)}{\Delta z(i+\frac12,j,k)}\right] \quad (2a)$$

$$P_r^{n+\frac12}(i+\tfrac12,j,k)=\frac{cr1(i+\frac12,j,k)}{cr2(i+\frac12,j,k)}P_r^n(i+\tfrac12,j,k)+\frac{1}{cr2(i+\frac12,j,k)}\left[cz2(i+\tfrac12,j,k)E_r^{n+\frac12}(i+\tfrac12,j,k)-cz1(i+\tfrac12,j,k)E_r^n(i+\tfrac12,j,k)\right]$$

$$P_r'^{n+\frac12}(i+\tfrac12,j,k)=P_r'^n(i+\tfrac12,j,k)+\left[crI2(i+\tfrac12,j,k)P_r^{n+\frac12}(i+\tfrac12,j,k)-crI1(i+\tfrac12,j,k)P_r^n(i+\tfrac12,j,k)\right]$$

For the second sub time step:

$$E_r^{n+1}(i+\tfrac12,j,k)=\frac{cz1(i+\frac12,j,k)E_r^{n+\frac12}(i+\frac12,j,k)-cr1(i+\frac12,j,k)P_r^{n+\frac12}(i+\frac12,j,k)}{cz2(i+\frac12,j,k)}+\frac{cr2(i+\frac12,j,k)\left[crI1(i+\frac12,j,k)P_r^{n+\frac12}(i+\frac12,j,k)-P_r'^{n+\frac12}(i+\frac12,j,k)\right]}{cz2(i+\frac12,j,k)crI2(i+\frac12,j,k)}+\frac{cr2(i+\frac12,j,k)P_r'^{n+\frac12}(i+\frac12,j,k)}{cz2(i+\frac12,j,k)crI2(i+\frac12,j,k)cm(i+\frac12,j,k)}+\frac{\Delta t\cdot cr2(i+\frac12,j,k)}{2\varepsilon\left(i+\frac12,j,k\right)\cdot cz2(i+\frac12,j,k)crI2(i+\frac12,j,k)cm(i+\frac12,j,k)}\left[\frac{H_z^{n+\frac12}(i+\frac12,j+\frac12,k)-H_z^{n+\frac12}(i+\frac12,j-\frac12,k)}{\phi\cdot(i+\frac12)\cdot r(i+\frac12)}-\frac{H_\phi^{n+1}(i+\frac12,j,k+\frac12)-H_\phi^{n+1}(i+\frac12,j,k-\frac12)}{\Delta z(i+\frac12,j,k)}\right]$$

$$P_r^{n+1}(i+\tfrac12,j,k)=\frac{cr1(i+\frac12,j,k)}{cr2(i+\frac12,j,k)}P_r^{n+\frac12}(i+\tfrac12,j,k)+\frac{cz2(i+\frac12,j,k)E_r^{n+1}(i+\frac12,j,k)-cz1(i+\frac12,j,k)E_r^{n+\frac12}(i+\frac12,j,k)}{cr2(i+\frac12,j,k)} \quad (2b)$$

$$P_r'^{n+1}(i+\tfrac12,j,k)=P_r'^{n+\frac12}(i+\tfrac12,j,k)+\left[crI2(i+\tfrac12,j,k)P_r^{n+1}(i+\tfrac12,j,k)-crI1(i+\tfrac12,j,k)P_r^{n+\frac12}(i+\tfrac12,j,k)\right]$$

where:

$$cr1(i+\tfrac12,j,k)=\kappa_r(i+\tfrac12,j,k)-\frac{\Delta t\cdot\sigma_r(i+\frac12,j,k)}{4\varepsilon_0}$$
$$cr2(i+\tfrac12,j,k)=\kappa_r(i+\tfrac12,j,k)+\frac{\Delta t\cdot\sigma_r(i+\frac12,j,k)}{4\varepsilon_0}$$
$$crI1(i+\tfrac12,j,k)=\kappa_r(i+\tfrac12,j,k)-\frac{\Delta t\cdot\int_{r_0}^{r}\sigma_r(r)dr}{4\varepsilon_0}$$
$$crI2(i+\tfrac12,j,k)=\kappa_r(i+\tfrac12,j,k)+\frac{\Delta t\cdot\int_{r_0}^{r}\sigma_r(r)dr}{4\varepsilon_0}$$
$$cz1(i+\tfrac12,j,k)=\kappa_z(i+\tfrac12,j,k)-\frac{\Delta t\cdot\sigma_z(i+\frac12,j,k)}{4\varepsilon_0}$$
$$cz2(i+\tfrac12,j,k)=\kappa_z(i+\tfrac12,j,k)+\frac{\Delta t\cdot\sigma_z(i+\frac12,j,k)}{4\varepsilon_0} \quad (2c)$$
$$cm(i+\tfrac12,j,k)=1+\frac{\Delta t\cdot\sigma(i+\frac12,j,k)}{2\varepsilon(i+\frac12,j,k)}$$

The expressions for other field components can also be obtained in the similar way.

The above formulation can solve the general media with arbitrary background conductivity and permittivity. The numerical grid can be nonuniform in all the three orthogonal directions.

III. NUMERICAL VERIFICATIONS

In this section, the cylindrical microstrip lines backed by a perfect conductor, as shown in Figure 1, are simulated. The ε_{eff} and Zo are computed with different W/H ratio. The large W/H ratio represents the thin-layer structure scenario. The outer radius b is 30.4mm, and the inner radius a 27.36mm (0.9b).

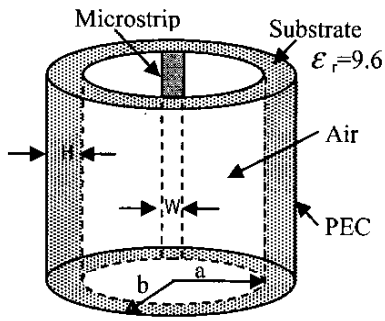

Fig. 1. Cylindrical Microstrip Line

(A) Gridding and Parameter Settings

Due to the removal of CFL condition, the ADI-FDTD time step can be selected independently from spatial steps. Consequently, a nonuniform mesh can be used without stability concerns. In our case, a grid nonuniform in both the radial and azimuthal diretions is applied. In the azimuthal direction, there are total 34 cells with 8 of them covering the microstrip line. In the radial direction, there are 5 cells within the substrate between the microstrip line and the perfect conductor. The thickness of the substrate varies from 0.304mm to 3.04mm, while the width of the microstrip line remains 3.04mm.

The UPML layers are added at both ends of the structure. The directional conductivity of σ_z in the UPML section is determined by [10]:

$$\sigma_z(z) = \sigma_{max}\left(\frac{z}{\delta}\right)^m \tag{3}$$

σ_{max} is the maximum conductivity of the UPML layer which, for the optimal performance, is recommended to be [10]:

$$\sigma_{max} = \sigma_{opt} = \frac{m+1}{150\,\pi\sqrt{\varepsilon_r}\,\Delta z} \tag{4}$$

In order to enhance the absorbing quality, parameter κ_z is chosen from 1 to κ_{max} from the interface [10]. κ_z for each layer is:

$$\kappa_z = 1 + \kappa_{max}\left(\frac{z}{\delta}\right)^m \tag{5}$$

The source is the Gaussian function added under the microstrip line. To eliminate the possible influence from higher order mode, the bandwidth of the Gaussian source is set to be 10 GHz, which is wide enough for quantitative analysis.

(B) Simulation Results

Table I shows the time-step applied. Δt_{FDTD}(ps) is the CFL limit that comes with the conventional FDTD. It is constrained by the spatial step. As H decreases, the cell size decreases. So does the Δt_{FDTD}(ps). However, the time-step with the ADI-FDTD is not limited by the condition. Therefore, it can be very large as long as the accuracy is maintained.

As can be seen in Table I, ADI-FDTD method is more efficient than conventional FDTD method, especially when W/H ratio is large or when the thin-layer structures are considered. The ADI-FDTD time step is hundreds to thousands times larger than the conventional FDTD time steps. Our numerical experience show that they amount to more than twenty times saving in CPU times.

Figure 2 and Figure 3 show the computed ε_{eff} and Zo in comparison to the results presented in [12]. They all agree well.

TABLE I Time step applied
with changing H and fixed W=3.04mm

W/H	$\Delta t_{ADI\text{-}FDTD}$(ps)	Δt_{FDTD}(ps)	$\Delta t_{ADI\text{-}FDTD}/\Delta t_{FDTD}$
1	1.32	8.59×10^{-3}	**153.6**
3	1.35	4.37×10^{-3}	**308.9**
7	1.36	1.83×10^{-3}	**742.5**
10	1.37	1.24×10^{-3}	**1103.5**
100	1.37	1.27×10^{-4}	**10797.8**

Finally, Fig. 4 shows the computed effective permittivities with different W/H ratios at 4.7 GHz. Again, the results computed with ADI-FDTD agree well with those presented in [12].

Due to the limit of space, the time-domain signatures of the waveforms are not presented. However they will be shown during the presentation.

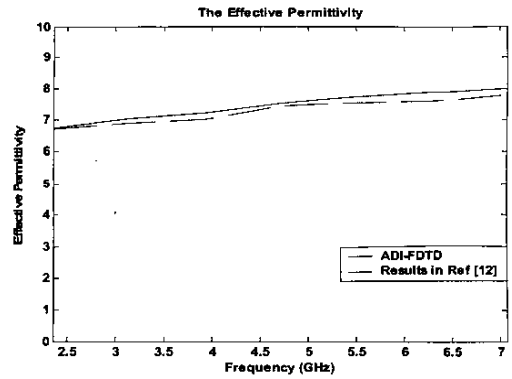

Figure 2 The effective permittivities with W/H=1

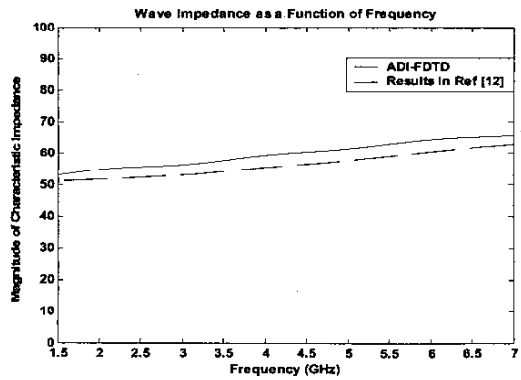

Figure 3 The characteristic impedances with W/H=1

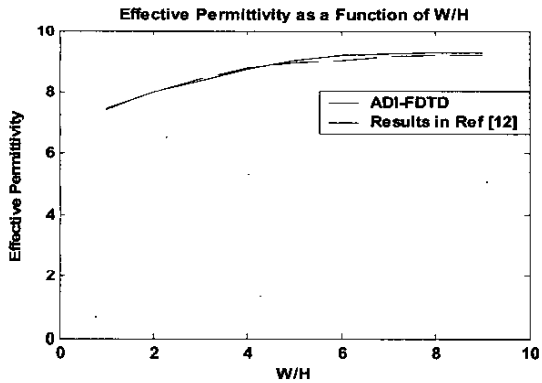

Figure 4 The effective permittivities with f=4.7 GHz

III. CONCLUSIONS

A cylindrical ADI-FDTD algorithm incorporated with the UPML absorbing boundary is presented for efficiently simulating thin-layer and open structures. The proposed unconditional stable method is found to be efficient and effective in computing the effective permittivities as well as characteristic impedances of cylindrical microstrip line with large W/H ratios.

The unconditional stable ADI-FDTD principle in this paper can be further extended to computing the non-cylindrical guided wave structures with very thin substrate or very narrow microstrip lines. It can be utilized for simulating thin multi-layer structures.

Acknowledgement

The authors acknowledge the financial support for this work from the National Science Research Council of Canada.

REFERENCES

[1] Taflove, *Computational Electrodynamics: The Finite-Difference Time-Domain Method*, Boston: Artech House, 1995.

[2] K. Chamberlin, and L. Gordon, "Modeling good conductors using the finite-difference time-domain technique" *IEEE Trans. Electromagnetic Compatibility*, vol. 37, pp. 210-216, May 1995.

[3] F. Zhen, Z. Chen, and J. Zhang, "Toward the development of a three-dimensional unconditionally stable finite-difference time-domain method," *IEEE Trans. Microwave Theo. Tech..*, vol. 48, pp. 1550-1558, September 2000.

[4] T. Namiki, "3-D ADI-FDTD method-unconditionally stable time-domain algorithm for solving full vector Maxwell's equations," *IEEE Trans. Microwave Theo. Tech.*, vol. 48, pp. 1743-1748, October 2000.

[5] F. Zheng and Z. Chen, "Numerical dispersion analysis of the unconditionally stable 3-D ADI-FDTD method", *IEEE Trans. Microwave Theo. Tech.*, vol.49,no 5,pp.1006–1009,May 2001.

[6] T. Namiki,; K. Ito, "Numerical simulation using ADI-FDTD method to estimate shielding effectiveness of thin conductive enclosures," *IEEE Trans. Microwave Theo. Tech.*, vol. 49, 1060-1066, June 2001.

[7] C. Yuan, Z.Chen, "Towards accurate time-domain simulation of highly conductive materials", *Digest of 2002 IEEE Inter. Microwave Symp.*, Seattle, WA, pp. 1335-1338, June 2002

[8] C. Yuan and Z. Chen, "On the modeling of conducting materials with the unconditionally stable ADI-FDTD method", under review for publication in *IEEE Transaction on Microwave Theo. and Tech.*

[9] C. Yuan, Z. Chen, "A three dimensional unconditionally stable ADI-FDTD method in the cylindrical coordinate system", *IEEE Trans. Microwave Theo. Tech.*, vol. 50, no. 10, pp. 2401-2405, October 2002.

[10] A. Taflove, *Advances in Computational Electrodynamics: The Finite-Difference Time-Domain Method*, Norwood, MA: Artech House, 1998.

[11] J. P. Berenger, "An efficient FDTD implementation of the PML with CFS in general media ", *Digest of IEEE Anten. and Propa. Society Inter. Symp.*, vol. 3, pp. 1362-1365, 2000

[12] R. Tsai, K. Wong, "Characterization of cylindrical microstriplines mounted inside a ground cylindrical surface", *IEEE Trans. Microwave Theo. Tech.*, vol. 43, no. 7, pp. 1607-1610, July 1995.